Journal of the European Ceramic Society **12** (1993) 309–314

Damage Characterization of a 2D SiC–SiC Composite Material

T. Despierres, M. Drissi Habti & M. Gomina
LERMAT, ISMRA, URA CNRS No. 1317, 6 Bvd Maréchal Juin, 14050 Caen Cedex, France

(Received 29 December 1992; revised version received 28 April 1993; accepted 30 April 1993)

Abstract

The damage characterization of a type of 2D SiC–SiC composite material made of Nicalon SiC fibres, a pyrocarbon interphase and a β-SiC matrix is conducted using uniaxial tensile tests. Damage is evaluated by the variations of the Young's modulus and the total number of cracks (either in the total volume of the specimen or only between the fibres inside the bundles) as functions of the applied strain, from the end of the linear behaviour to failure. It is shown that the Aveston, Cooper & Kelly model commonly used for the interfacial shear stress estimation is not applicable to this material.

Die Beschädigung von einer SiC–SiC 2D Verbundwerkstoffsorte, die aus SiC Nicalon Fasern, einer Kohlenstoffzwischengrenze und einer β-SiC Matrix besteht, wurde unter einachigem Zug untersucht. Die Änderungen des Elastizitätsmodul, der gesamten Anzahl von Mikrotissen (sowohl im Volumen der Probe als in den Faserbündeln) sind als Funktion der Verformung, vom Ende des linearen Bereichs bis zum Bruch, vorgetragen. Es stellt sich heraus, daß die Methodik von Aveston, Cooper & Kelly es nicht erlaubt, die Scherspannung an der Zwischengrenze zu bestimmen.

L'endommagement d'une nuance de matériaux composites SiC–SiC 2D constitués de fibres SiC Nicalon, d'une interphase de carbone et d'une matrice β-SiC est étudié à l'aide d'essais de traction uniaxiale. Les variations du module d'élasticité, du nombre total de fissures créées (aussi bien dans le volume total de l'éprouvette que seulement dans les torons de fibres) sont présentées en fonction de la déformation, depuis la fin du comportement linéaire élastique jusqu'à la rupture. Il s'avère que la méthode de Aveston, Cooper & Kelly ne permet pas l'estimation d'une contrainte de cisaillement interfacial dans ce type de matériau.

1 Introduction

Great attention is now focused on the development of high-temperature engineering ceramics with high levels of reliability, the most efficient of which are designed for heat engine components (ramjet and rocket engines chambers, hot gas valves, tubes, turbine wheels, etc.) and aerospace parts (Hermes space plane leading edges, body protection panels, nose, etc.). In these advanced materials continuous ceramic fibres (C, SiC) are used to confer damage tolerance capability on a ceramic matrix (C, SiC, Si_3N_4). It has been shown that these high toughness ceramic matrix composites (CMC) with extended *R*-curve behaviour at room temperature are obtained when the fibre/matrix interface gained from the matrix process or introduced before the matrix deposit is sufficiently weak. This requirement is hardly encountered when chemical bonds are present between the fibre and the matrix during processing: weak interfaces are associated with mechanical interactions due to the difference between the coefficients of thermal expansion (CTE) of the fibre and the matrix, and to the irregularities on the surface of the fibre.

Nowadays the key point in the processing of tough ceramic fibre-reinforced ceramic matrix composites is the control of the fibre/matrix bonding by means of a thin layer of a compliant material (the interphase).[1–4] The function of this layer is mainly to prevent the failure of the fibres in mode I by direct propagation of a crack initiated in the brittle matrix: such a crack must be deflected along the fibre, creating fibre/matrix debonding, post-debonding friction and extensive fibre pull-out. As these materials are aimed to be used for parts operating under high temperatures and different gaseous environments,[5,6] it is essential to afford a reliable testing apparatus (grips, alignment system) for the evaluation of damage in relation with the applied strain.

Journal of the European Ceramic Society 0955-2219/93/$6.00

In this paper a damage investigation in terms of the variation of the Young's modulus as a function of the deformation of the specimen is presented. It is also analysed in terms of the variation of the total number of cracks in the volume of the specimen or only in the fibre bundles (to check the applicability of the Aveston, Cooper & Kelly (ACK) model for interfacial shear stress evaluation[7,8]) lying parallel to the stress direction, as a function of the strain.

2 Experimental Procedure

2.1 Materials

The materials under test are SiC–SiC ceramic composites made of equilibrated woven tissue of SiC Nicalon fibres (NLM 202 type) stacked and covered with a thin layer (0·05–0·1 μm) of pyrocarbon.[9,10] The physical properties of these orthotropic materials include a Young's modulus $E_c = 230$ GPa, an ultimate tensile stress $\sigma_r = 180$ MPa, a density of 2·5–2·6 g cm^{-3} and a strain to rupture $\varepsilon_r \simeq 0{\cdot}20\%$ (as given by the manufacturer, SEP, Bordeaux). In these materials the matrix is much stiffer than the fibres ($E_m = 390$ GPa, $E_f = 200$ GPa) and remains in tension at room temperature as a consequence of the difference in the thermal expansion coefficients ($\alpha_f = 3 \times 10^{-6}$ and $\alpha_m = 4{\cdot}6 \times 10^{-6}$°C^{-1}) of the constituents of the materials.[11,12]

2.2 Experimental tests

The tensile specimens are dogbone-shaped specimens with the principal axis parallel to a direction of reinforcement, cut from an unprotected plate. The fracture around the grips was hindered by the selection of appropriate geometry and dimensions of the test piece. The gauge length is 40 mm with a cross-sectional area of 8 × 3 mm^2, the total length of the specimen is 120 mm.

The specimen alignment to prevent bending and torsion moments introduced by the tensile load train was assured using new mechanical grips specifically designed by the Schenck Company (Darmstadt, Germany) for these types of materials (Fig. 1). These compact and very light grips have been given a triaxial rotation capability with the centres of rotation located at the loading points on the central line of the testing machine. The pre-strained clamping cylinders with a special surface treatment should be used for alternating loading and fatigue tests up to 1700°C.

The tensile strain was measured directly on the gauge section of the specimen using an axial strain transducer DSA of gauge length 25 mm and 2·5 mm of nominal displacement, while the tests were run at a cross-head speed of 50 μm min^{-1} on a Schenck RMC-type machine equipped with a 100 KN load cell.

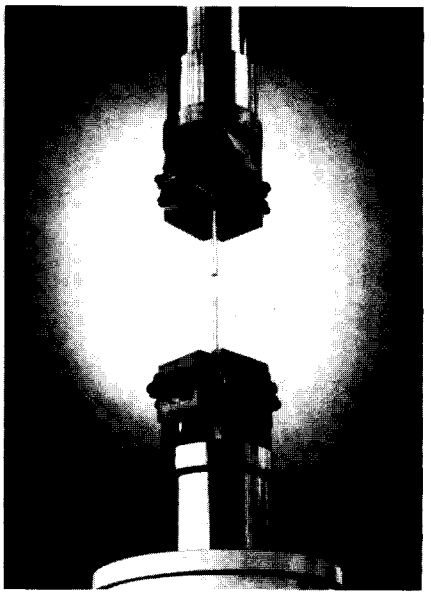

(a)

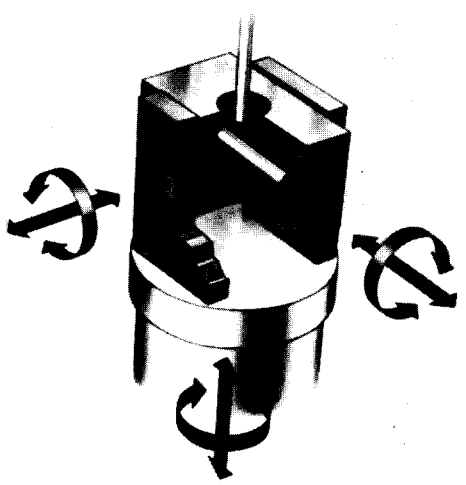

(b)

Fig. 1. (a) General and (b) schematic view of the mechanical grips used for static tension, compression and for fatigue tests with alternating loading.

A typical stress–strain curve up to rupture of a 2D SiC–SiC tensile specimen is shown in Fig. 2. Using this curve, identical specimens were loaded at different strain values, ε. The damage induced in the specimens is then estimated by the number of cracks in the matrix revealed when using Murakami's reactant. The total number of cracks in the gauge length was documented by in-situ scanning electron microscope observations only in the fibre bundles lying parallel to the applied stress direction (Section 3.3) or in the total calibrated volume of the specimen (Section 3.2). The mean distance between two successive cracks $\langle l \rangle$ and the distance $\langle d \rangle$ obtained by dividing the gauge length by the total number of cracks was also analysed.

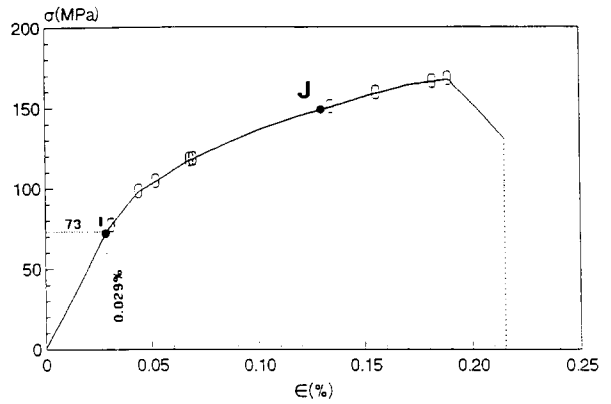

Fig. 2. Typical stress–strain curve of a 2D SiC–SiC specimen (——) showing at which locations the specimens were strained for damage evaluation (○).

3 Results and Discussion

3.1 General observations

The loading curve in Fig. 2 can be described as follows:

(i) First, a linear behaviour of the specimen is observed, which extends from the origin O to the point I ($\varepsilon_I = 0{\cdot}035\%$, $\sigma_I = 80$ MPa). The measured Young's modulus $E_0 = 220$ GPa is the same as the one estimated using the rule of mixtures with the fibres parallel to the stress direction (an effective volume fraction of fibres $V'_f = V_f/2 = 20\%$ was assumed). But the first cracks in the matrix appear at a low strain level ($\varepsilon_e = 0{\cdot}029\%$, $\sigma_e = 73$ MPa) before the end of the linear behaviour.

(ii) The second zone (from I to J) is characterized by a progressive increase in the number of microcracks in all the calibrated volume of the specimen.

(iii) In the third zone where the fibres break progressively, the tangent modulus is somewhat constant ($E_s = 36$ GPa). When assuming this value to be the stiffness of the remaining fibres, the application of the rule of mixture gives a value $V''_f = 18\%$: that means 10% of the initial effective volume fraction of fibres have failed. This zone extends from $\varepsilon_s = 0{\cdot}13\%$ to the ultimate strain ε_r.

Scanning electron microscopy observations reveal that the cracks initiate preferably from the sharp angles of the macroporosities resulting from the woven structure of the material. Thereafter the cracks propagate in mode I in the matrix through the total thickness of the specimen.

3.2 Damage evaluation in the volume as function of the applied strain

For different values of the strain, the total number of transverse cracks N_v in the specimen and their position along the gauge length are depicted in Fig. 3(a)–(f). The cracks are equally distributed in the gauge length and it appears (Fig. 4(a) and (b)) that both parameters N_v and $\langle d \rangle$ (or $\langle l \rangle$) reach a saturation level (71 and 570 μm respectively) for strains above $\varepsilon_s = 0{\cdot}13\%$, that is, an applied stress level of 149 MPa.

In the case of unidirectional composites, the saturation in the mean distance between the cracks in the volume of the specimen allows the calculation of the interfacial shear stress τ, using the ACK model. But, for the materials with a 2D woven structure, the microcracking pattern in the volume of the specimen is not representative of the stress transfer from the fibres to the matrix. Thus the saturation level shown in Fig. 4(b) may not be used for the evaluation of τ.

Meanwhile, the prediction of the variation of N_v as function of ε is of interest, especially when the material is used in an environment where the stripped fibres can be corroded.

3.2.1 Kinetics of the increase in the total number of cracks

It has already been shown that the damage in the specimens can be expressed by the total number of transverse cracks N_v (Fig. 4(a)). The increase in the number of cracks as a function of the strain suggests a similarity with a growth process governed by a chemical-like kinetic:

$$\frac{dN}{dt} = \frac{dN}{d\varepsilon} * \frac{d\varepsilon}{dt} = k(N_s - N) \tag{1}$$

which can be solved for

$$N = N_s[1 - \exp(-\beta(\varepsilon - \varepsilon_0))] \tag{2}$$

where ε_0 is the strain at the end of the linear behaviour of the safe specimen.

In Fig. 5 the results from eqn (2) fit the experimental values for $\beta = 27{\cdot}9$ and thus this expression is quite a good predictive law for damage evaluation as a function of the applied strain.

3.2.2 Residual elastic modulus as damage parameter

Until now, damage in the specimens has been given in terms of the total number of transverse cracks in the matrix. However, the residual elastic modulus is the most easily and directly measurable parameter. The specimen strained to a level ε is unloaded and then reloaded for the measurement of the elastic modulus from the compliance obtained on the reloading loop (Fig. 6). These E values, plotted in Fig. 7(a) as a function of the applied strain, exhibit an exponential-type dependence:

$$E = E_0 \exp[-\alpha(\varepsilon - \varepsilon_0)] \tag{3}$$

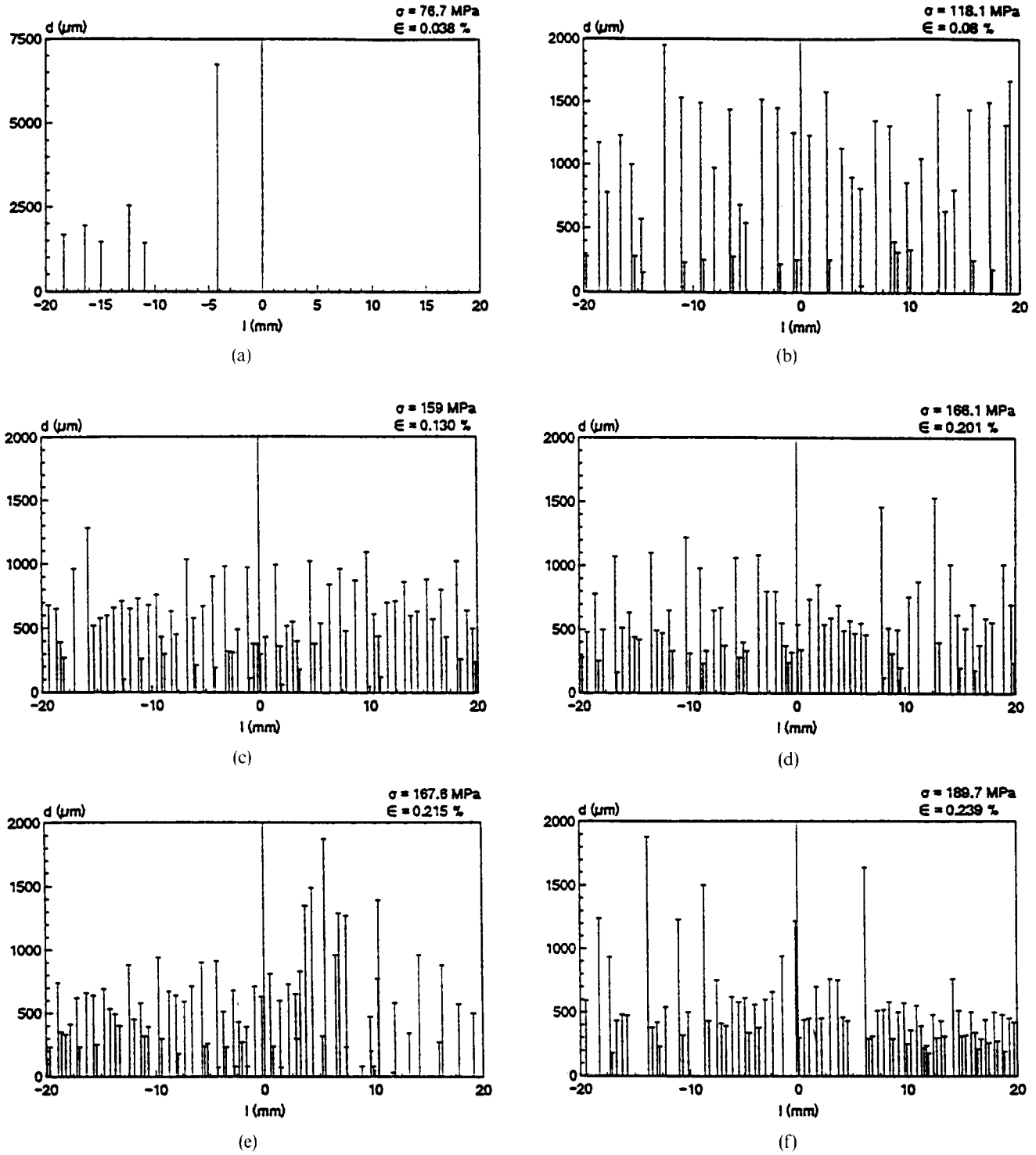

Fig. 3. Distribution of the distance between successive cracks in the gauge length for different strain levels.

with $\alpha = 5{\cdot}54$ (Fig. 7(b)), ε_0 is the strain at the end of linear behaviour of the safe specimen.

The representation of these E values as a function of the number of cracks N_v shows a continuously decreasing relationship (Fig. 7(c)) useful for the prediction of microcracking when the specimen is constrained.

The meaning of the parameters α and β is not yet clear, but they should be related to any micromechanical properties of the basic constituents, the geometry of the reinforcement and of the fibre/matrix interface.

3.3 Damage evaluation in the fibre bundles

For the specimens already discussed, the total number of cracks in the matrix inside the fibre bundles (N_b) has been monitored (Fig. 8). N_b increases continuously with the strain level up to rupture (Fig. 9). The total number of transverse cracks inside the individual bundles (N_b) is much higher than in the bulk of the specimens (N_v) as a consequence of the stress transfer mechanism from the fibres to the matrix through the interfacial shear stress.

Inside the bundles, the mean distance between

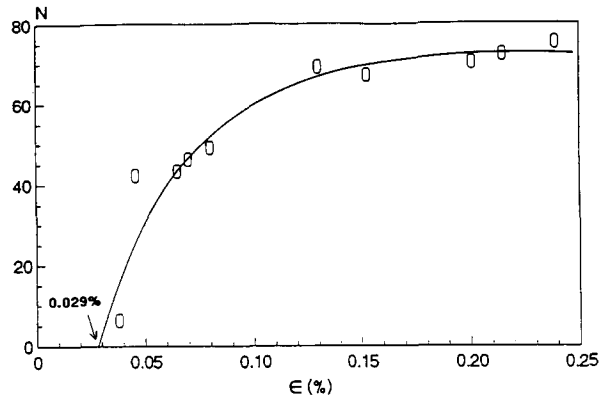

(a)

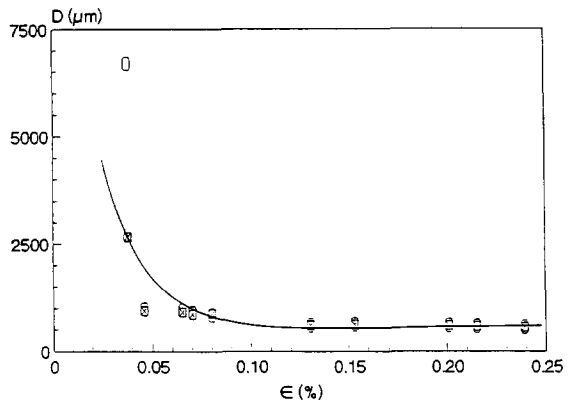

(b)

Fig. 4. (a) Total number of transverse cracks in the matrix as a function of the strain level. (b) Mean spacings between transverse cracks in the matrix as a function of the strain level: ⊗, $\langle l \rangle$; ○, $\langle d \rangle$ (see the text for the meaning of $\langle d \rangle$ and $\langle l \rangle$).

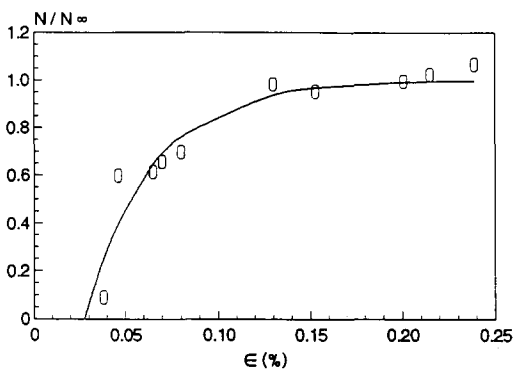

Fig. 5. Evolution of the total number of cracks in the volume as a function of the strain. ——, N/N_∞ calculated; ○, N/N_∞ measured.

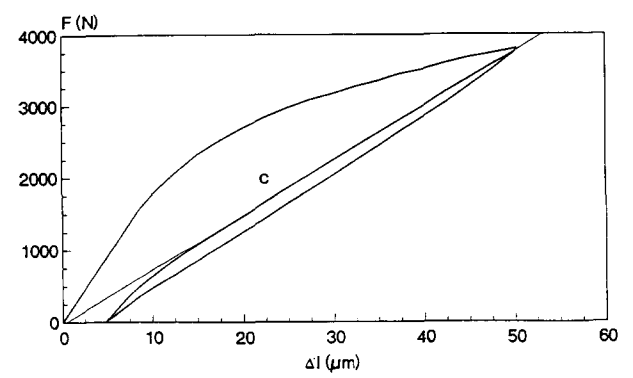

Fig. 6. Schematic diagram of the compliance measurement on the reloading loop.

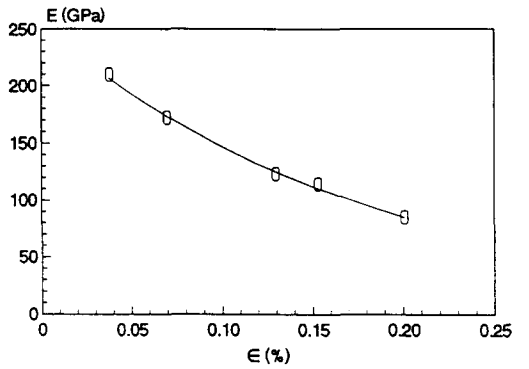

(a)

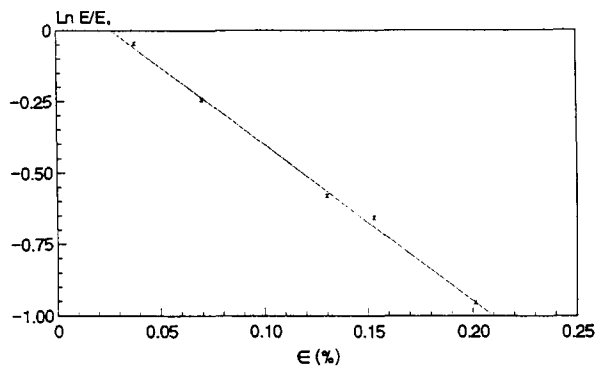

(b)

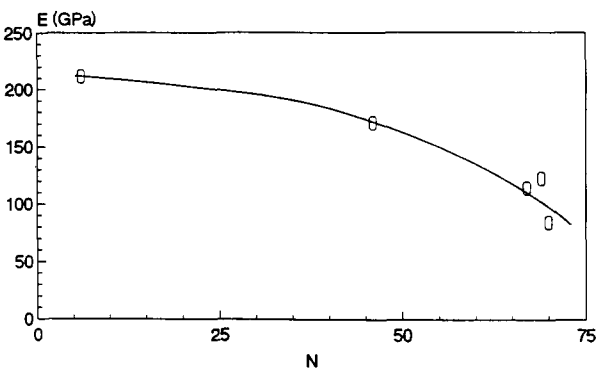

(c)

Fig. 7. (a) Evolution of the Young's modulus as a function of the applied strain: ——, E calculated; ○, E measured. (b) ln E/E_0 as a function of ε for the determination of the exponent α. (c) Residual Young's modulus E as a function of the total number of cracks N_v.

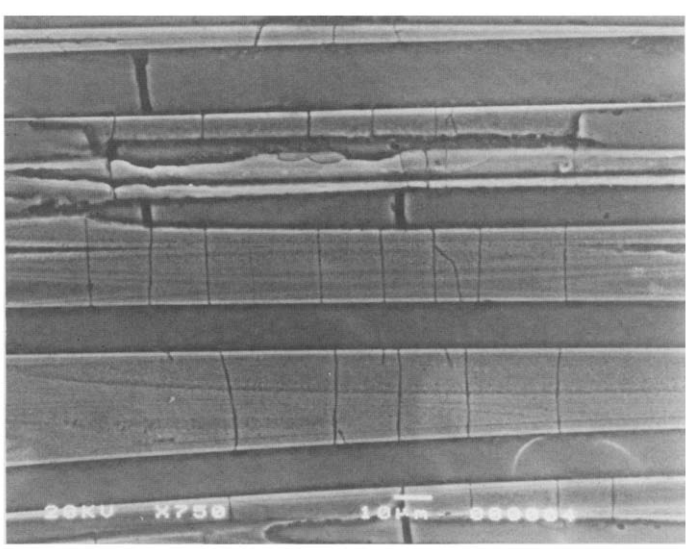

Fig. 8. Microcracks pattern inside the bundle.

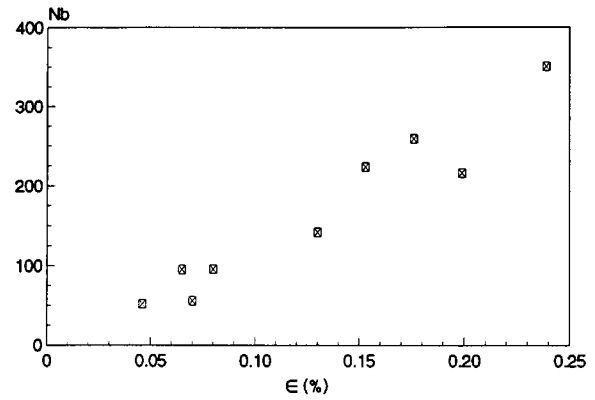

Fig. 9. Evolution of the total number of cracks in the bundles, N_b, as a function of the applied strain.

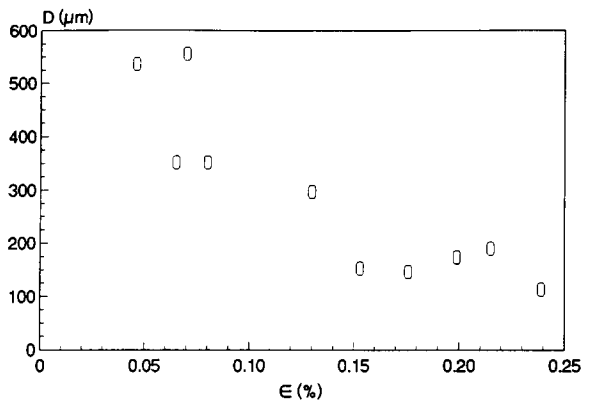

Fig. 10. Mean intercrack spacing between transverse cracks in the bundles as a function of the strain level.

successive cracks $\bar{d}$ decreases rapidly for $\varepsilon < 0{\cdot}10\%$ (Fig. 10). However, $\bar{d}$ does not reach a saturation level, as assumed in the ACK model for the interfacial shear stress evaluation. This results from any structural singularities of the materials: the low Weibull modulus of the Nicalon SiC fibres after the elaboration process of the composite ($m = 3$–4), the pores in the matrix and the irregularities at the fibre/matrix interfaces which hinder a good stress transfer from the fibres to the matrix. Thus the ACK model may not be used to work out an interfacial shear stress value for these composites.

4 Conclusions

Damage evaluation in a 2D SiC–SiC material has been performed using a specially designed tensile loading train suitable for ceramics. The damage level has been evaluated in terms of the evolution of the Young's modulus E and of the total number of cracks in the bulk of the specimens (N_v) and inside the bundles of fibres (N_b), as functions of the applied strain. The ACK model may not be applied to this 2D SiC–SiC ceramic composite because no saturation level appears in the evolution of the mean crack interspacing as a function of the strain level. The variation of N_v and E with the strain level are dependent on two parameters β and α respectively which should be related to the physical properties of the constituents and the geometry of the reinforcement of the material under study.

Acknowledgements

This work has been mainly supported by the Scientific Group GS Composites Thermostructuraux created by Centre National de la Recherche Scientifique (CNRS) and Société Européenne de propulsion (SEP), France.

References

1. Joste, B., Observations en MET de matériaux composites SiC–SiC. Relations d'orientation dans les matériaux SiC–SiC, Project Report at ISMRA Engineer School, Caen, 1986.
2. Lowden, R. A. & Stinton, D. P., The influence of the fiber/matrix bond on the mechanical behaviour of Nicalon/SiC composites, Oak Ridge (Tenessee): Oak Ridge National Laboratory, Report No. ORNL/TM-10667, DE88006155, 1987.
3. Maniette, Y., Contribution à l'étude de phénomènes d'interphases dans des composites de carbure de silicium. Thèse de Docteur–Ingénieur, Université de Pau et des Pays de l'Adour, 1988.
4. Lowden, R. A. & Stinton, D. P., Interface modification in Nicalon/SiC composites. *Ceram. Eng. Sci. Proc.*, **9**(7–8) (1988) 705–22.
5. Fourvel, P., Silvestrini, P., Rouillon, M. H., Vicens, J. & Gomina, M., Structural modifications of a SiC–SiC material exposed at high temperature in air. *J. Mater. Sci.*, **25** (1990) 5163–5.
6. Gomina, M., Fourvel, P. & Rouillon, M. H., High temperature mechanical behaviour of SiC–SiC composite materials. In *The Proceedings of the First European Ceramic Society Conference*, 18–23 June 1989, Maastricht, The Netherlands, Vol. 3, ed. G. de With, R. A. Terpstra & R. Metselaar. Elsevier Applied Science, London and New York, 1989, pp. 366–71.
7. Aveston, J., Cooper, G. A. & Kelly, A., Single and multiple fracture. *Proc. Conf. The Properties of Fibre Composites.* IPC Science and Technology Press, Guildford, UK, 1971, pp. 15–26.
8. Aveston, J. & Kelly, A., Theory of multiple fracture of fibrous composites. *J. Mater. Sci.*, **8** (1973) 352–62.
9. Monthioux, M., In a Report from Laboratoire Marcel Mathieu, UMR 124-CNRS in Groupement Scientifique Comportement Thermomécanique de Composites Céramiques–Céramiques supported by CNRS and SEP, France, 1991.
10. Bouillon, M. H., Mocaer, D., Villeneuve, J. F., Naslain, R., Monthioux, M., Oberlin, A., Quimon, C. & Pfister, G., Composition–microstructure–property relationships in ceramic monofilaments resulting from the pyrolysis of a polycarbosilane precursor at 800 to 1400°C. *J. Mater. Sci.*, **26** (1991) 1517–30.
11. Naslain, R., Two-dimensional SiC/SiC composites processed according to the isobaric–isothermal vapor infiltration gas phase route. In *The Proceedings of the 5e Rencontre Marocaine sur la Chimie de l'Etat Solide (REMCES V)*, Casablanca, 30 October–1 November, *J. Alloys Compounds*, **188** (1992) 42–8.
12. Madigou, V., Characterisation of ceramic composites and their constituents: precursors, fibres and interphase, *Microsc. Microanal. Microstruct.*, **2** (1991) 47–57.